ChemComm

COMMUNICATION

View Article Online
View Journal | View Issue

Cite this: *Chem. Commun.*, 2025, **61**, 10138

Received 26th February 2025,
Accepted 5th June 2025

DOI: 10.1039/d5cc01040c

rsc.li/chemcomm

Pseudorotaxane monolayers of pillar[5]arene and linear fatty acids at the air–water interface†

Masaki Ishii, *[ab] Yuto Nakai,[ab] Yu Yamashita,[a] Katsuto Onishi,[c] Tan-hao Shi,[c] Nobutaka Shioya,[d] Hideki Sakai,[b] Takeshi Hasegawa,[d] Tomoki Ogoshi,[ce] Katsuhiko Ariga[abf] and Taizo Mori[d]

Pseudorotaxanes, which are formed by macrocyclic host molecules and linear guest molecules, show potential in molecular devices and surface applications. In this study, ethoxy-functionalized pillar[5]arene (P5A) and amphiphilic linear fatty acid guests were self-assembled into oriented monolayers at the air–water interface. The fatty acid structure dictates the monolayer formation: [2]pseudorotaxane-based, [3]pseudorotaxane-based and phase-separated monolayers. These findings provide insights into P5A-based pseudorotaxane monolayers, facilitating their integration into advanced functional materials.

Pseudorotaxanes are formed by a macrocyclic host molecule and a linear guest molecule that exhibits specific non-covalent interactions with the host.[1] The tiling of oriented pseudorotaxanes particularly in two-dimensional planes is promising for applications such as molecular shuttles,[2,3] surface wettability control,[4] sensors,[5] catalysts,[6] and transistors.[7] Compared with the commonly used self-assembled monolayer (SAM) method for surface modification, the Langmuir--Blodgett (LB) technique[8] imposes significantly fewer material limitations because of the lack of chemical bonds between the pseudorotaxane terminal functional groups and the substrate surface. Additionally, this method allows for control of the density and orientation of pseudorotaxanes through in-plane mechanical compression.

Pillararenes, first developed in 2008,[9] are a class of macrocyclic host molecules, with cyclopentamer (P5A) and cyclohexamer (P6A) derivatives being the most commonly used. Compared to other macrocyclic host molecules, such as crown ethers and calixarenes, pillararenes offer advantages in terms of easy synthesis, flexible functionality, and high symmetry.[10] In particular, P5A forms pseudorotaxanes with saturated alkanes *via* C–H$\cdots\pi$ interactions.[11,12] Recent studies have demonstrated that P5A-based pseudorotaxanes can exhibit bistable states,[13,14] offering applications such as molecular machines, similar to those investigated in "blue box" systems.[3] Accordingly, two-dimensional tiling of P5A-based pseudorotaxanes can maximize the expression of switchable surface functionalities. Therefore, understanding P5A-based pseudorotaxane monolayers at the air–water interface is expected to open new avenues for various applications.

In this study, we found that pseudorotaxanes, which is composed of ethoxy-functionalized pillar[5]arene (EtP5A) and linear fatty acid guests, were oriented and assembled in a monolayer at the air–water interface. The chemical structure of the fatty acid guest dictates the resulting monolayer structure; short-chain linear fatty acids lead to [2]pseudorotaxane monolayers, long-chain linear fatty acids form [3]pseudorotaxane monolayers, and a fatty acid guest unsuitable for EtP5A undergoes phase separation (Fig. 1a).

To elucidate the monolayer state of Langmuir films at the air–water interface, we measured the surface pressure–area (π–A) isotherms (Fig. 1b). Pure EtP5A exhibited a lift-off of the surface pressure near 1.3 nm^2 and monolayer collapse at 10.3 mN m^{-1}. Interestingly, given the good agreement with the theoretical calculations (1.42 nm^2), the pure EtP5A with simple ethoxy substitution was found to orient its cavities perpendicular to the water surface, as observed in previous studies using pillararene with longer and more complex substitution.[15,16] The relatively low collapse pressure (π_C) suggested weak intermolecular interactions within the plane. To obtain a stable and oriented pseudorotaxane monolayer, we mixed a chloroform solution with amphiphilic G5-18, which has been widely employed in insoluble monolayer studies.[8,17] Mixing with G5-18 at a molar ratio of 1 : 1 decreased the limiting cross-sectional area (A_L) per EtP5A molecule from 1.28 nm^2 to 0.91 nm^2, as

[a] *Research Center for Materials Nanoarchitectonics (MANA), National Institute for Materials Science (NIMS), Tsukuba, Ibaraki, Japan*
[b] *Graduate School of Science and Technology, Tokyo University of Science, Noda, Chiba, Japan. E-mail: 7221701@ed.tus.ac.jp*
[c] *Graduate School of Engineering, Kyoto University, Nishikyo-ku, Kyoto, Japan*
[d] *Institute for Chemical Research, Kyoto University, Uji, Kyoto, Japan*
[e] *WPI Nano Life Science Institute, Kanazawa University, Kakuma-machi, Kanazawa, Japan*
[f] *Graduate School of Frontier Science, The University of Tokyo, Kashiwa, Chiba, Japan*

† Electronic supplementary information (ESI) available. See DOI: https://doi.org/10.1039/d5cc01040c

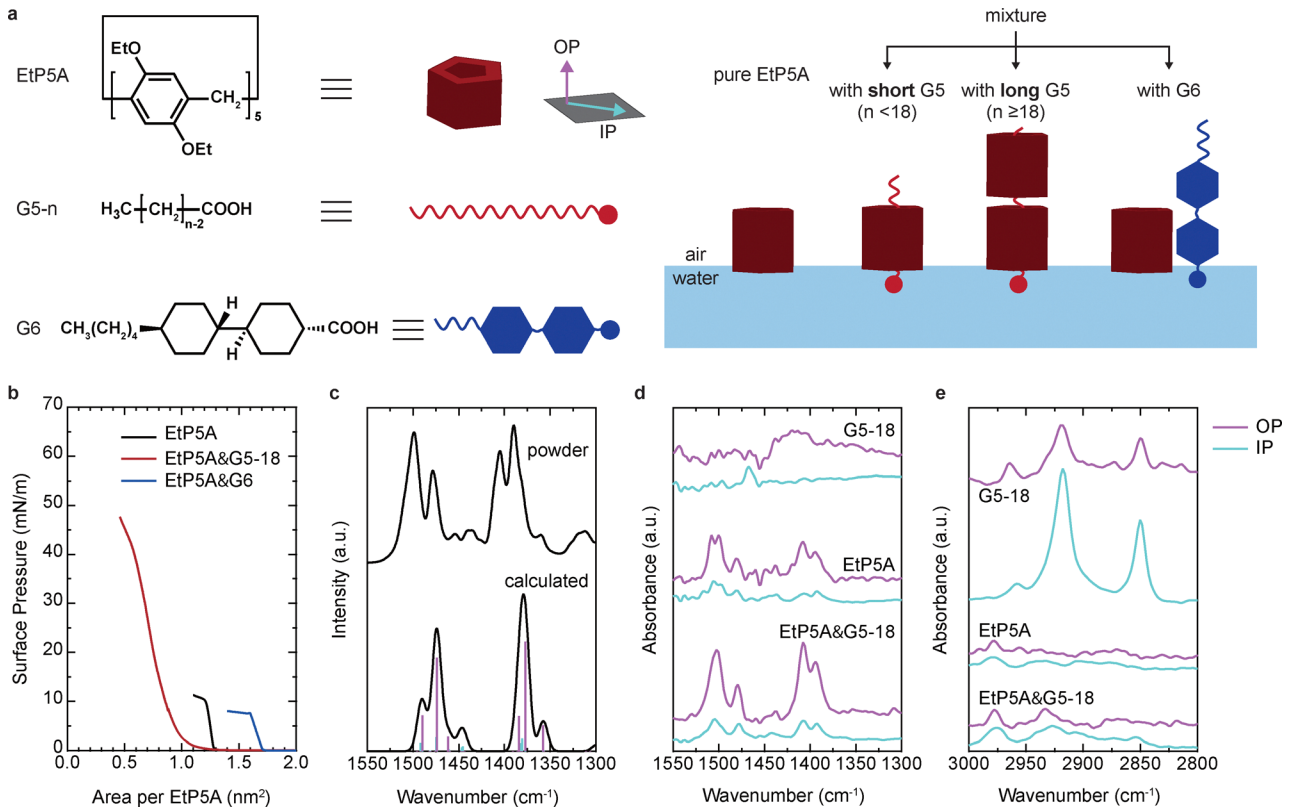

Fig. 1 Pseudorotaxane of EtP5A at the air–water interface. (a) Molecular structures and schematics of monolayer states for employed EtP5A host and guests. (b) π–A isotherms for pure EtP5A (black line), mixture with G5-18 (red line) and with G6 (blue line). (c) DFT-calculated IR spectrum of EtP5A with experimental one of the powder (Section 1.4, ESI†). MAIRS spectra of LB films for pure EtP5A, mixture with G5-18 and pure G5-18 in the 1550–1300 cm^{-1} (d) and 3000–2800 cm^{-1} (e) regions. The OP (pink line) and IP (light blue line) indicate the out-of-plane and in-plane directions of the LB films, respectively.

calculated by extrapolating the π–A isotherms. The reduction in molecular area by as much as 0.37 nm^2 does not occur if EtP5A and G5-18 form no complexes or 1 : 1 complexes, suggesting the formation of [3]pseudorotaxane structure at the air–water interface. Note that the A_L per EtP5A molecule of 0.91 nm^2 is close to the sum of one-half of the A_L of 1.28 nm^2 for a single PA molecule and the A_L of 0.2 nm^2 for an alkyl chain, which support [3]pseudorotaxane formation. Furthermore, the [3]pseudorotaxane structure might contribute to the formation of a more in-plane rigid film as confirmed by the significant increase in π_C of 43.2 mN m^{-1} compared to 10.3 mN m^{-1} of pure EtP5A. On the other hand, when mixed with G6, a guest molecule incompatible with the cavity size of EtP5A, π–A isotherm shifted toward larger molecular areas corresponding to the cross-sectional area of G6, with minimal changes in π_C compared to pure EtP5A. This behavior indicates phase separation within the two-dimensional film.[18] Similar phase separation was observed when EtP5A and G5-18 were sequentially spread on the water surface (Fig. S6, ESI†). Note that host–guest chemistry strongly influences these phenomena, as demonstrated by the formation of pseudorotaxanes with G6 and phase separation with G5 when using EtP6A as the host (Fig. S7, ESI†).

To investigate the molecular orientation and pseudorotaxane formation, we performed multiple-angle incidence resolution spectroscopy (MAIRS) measurements on LB films transferred from the water surface. This method involves tilting the thin film relative to the optical axis and analyzing the infrared absorption spectra acquired at varying polarization angles.[19] The MAIRS method can separate the out-of-plane (OP) and in-plane (IP) absorption components of the film materials. Unlike traditional approaches that combine transmission and reflection methods,[17] the MAIRS method offers the advantage of measuring one identical film with fewer substrate constraints. EtP5A exhibited similar absorption characteristics in both the powder and LB films (Fig. 1c and d). According to density functional theory (DFT) calculations, the most intense absorption bands at 1502 cm^{-1} and 1408 cm^{-1} were mainly consisted of aromatic C–H bending, aromatic C–H stretching, CH_2 wagging, and CH_3 wagging vibrations (Section 1.4, ESI†). The strong transition moments along the cavity direction of EtP5A can be useful for assessing the molecular orientation. For both LB films of pure EtP5A and the mixture of EtP5A and G5-18, these vibrational bands were more prominent in the OP spectrum than in the IP spectrum, indicating the vertical orientation of the EtP5A cavity, both at the air–water interface and after transfer to solid substrates. This vertical orientation of EtP5A corresponds to the fact that the A_L obtained by π–A isotherm is close to the calculated cross-section value of

1.42 nm^2 for pure EtP5A. Additionally, pure G5-18 exhibited characteristic vibrational peaks due to CH_2 *trans*-zigzag packing owing to its crystallinity, specifically CH_2 antisymmetric stretching vibrations (2920 cm^{-1}) and CH_2 symmetric stretching vibrations (2850 cm^{-1}) (Fig. 1e).[20,21] Upon mixing with EtP5A, these peaks shifted to higher wavenumbers, indicating that the alkyl chains adopted a *gauche* conformation and supporting the formation of inclusion complexes with EtP5A.

Considering that the formation behavior of EtP5A-based pseudorotaxanes depends on the chain length of the guest molecules,[12] the monolayer state was investigated using guests with carbon numbers ranging from 14 to 26, which can independently form insoluble monolayers. In this study, the molecules were mixed at a 1 : 1 molar ratio before spreading to the air–water interface. The π–A isotherms for each system, guest-dependent A_L, and guest-dependent collapse areas and π_C are shown in Fig. 2a, b, and c, respectively. All the molecular areas were calculated per EtP5A molecule. Compared to pure EtP5A, the π_C for all mixed systems increased, suggesting that pseudorotaxane formation and concomitant lateral hydrophobic interactions between alkyl chains improved monolayer rigidity. The constant A_L and π_C indicate that EtP5A forms a nearly identical two-dimensional film when mixed with guests having carbon numbers greater than 18, where [3]pseudorotaxane is stabilized as discussed later. In contrast, the mixed systems with G5-14 and G5-16 exhibited larger A_L and lower π_C than those with G5-18 and other guests. Note that a similar collapse area of 1.20 nm^2 for pure EtP5A and the mixture with G5-14 implies that the mixed system mainly consists of a 1 : 1 complex, that is, [2]pseudorotaxane. The gradual shift in the A_L with increasing carbon number indicates that the stoichiometry of pseudorotaxane formation depends on the carbon number of the guest molecules.[12] In other words, it is plausible that the composition of the monolayers—[2]pseudorotaxane, [3]pseudorotaxane, and uncomplexed molecules—varies depending on the type of guest molecule, given that the π–A isotherms provide average information about the Langmuir films on the water surface, which extend over an area of several hundred cm^2.

To assess the effect of the molecular mixing ratio, we analyzed π–A isotherms for a mixture with G5-20, which has a sufficiently long carbon chain to stabilize the monolayer state, as shown in Fig. 2b and c. Here, when n_A represents the number of molecules of A, the host–guest stoichiometric ratio (SR) is defined as n_{G5}/n_{EtP5A} in the mixing solution. The horizontal axis in Fig. 3a and the A_L in Fig. 3b are plotted against the area per EtP5A molecule. Given that the collapse behavior of Langmuir films depends on the compressibility of the entire film, the collapse area is represented as a mean value for all mixed molecules (Fig. 3c). As expected, π–A plots approached the characteristics of pure EtP5A (or pure G5-20) as the stoichiometric ratio approached zero (or infinity) (Fig. S9, ESI†). Interestingly, the A_L per EtP5A molecule and the collapse behavior exhibited a clear bifurcation at a stoichiometric ratio of 3/7. Within each of the two groups, the A_L can be approximated by a linear trend with an intersection of approximately 0.33. The decrease in the molecular area of binary Langmuir films is often indicative of specific attractive interactions.[8,22] In this system, such a trend strongly suggests pseudorotaxane formation. Assuming that all G5-20 molecules participate in complex formation under excess conditions of EtP5A (*e.g.*, SR = 1/9, 2/8, 3/7), the number of EtP5A molecules involved in each pseudorotaxane can be estimated from the A_L. The results are 2.1, 2.3, and 2.0 EtP5A molecules, respectively, strongly indicating that [3]pseudorotaxane is the dominant species in the mixed monolayer films. Conversely, under conditions where G5-20 is in excess, the decrease in area surpasses the value expected from molecular interactions associated with pseudorotaxane formation, making it challenging to describe the behavior with a simple additivity rule. Further investigations are necessary to elucidate this phenomenon. Nonetheless, the identical collapse behavior implies that the monolayers include [3]pseudorotaxane.

In conclusion, we systematically investigated monolayers of ethoxy-substituted P5A and mixtures with fatty acid guests. Linear fatty acid guests lead to pseudorotaxane monolayers with P5A cavities oriented toward the water surface. The mixing ratio and chain length of the guests influenced the stoichiometry of pseudorotaxane formation and monolayer composition. This study provides insight into P5A-based pseudorotaxane monolayers for various applications. The simple procedure employed for monolayer formation also offers the possibility of introducing functional properties by appropriately selecting host and guest molecules. Furthermore, by removing guest molecules after the formation of aligned pseudorotaxane films, these materials can be explored for applications in sensors and filters.[23–25]

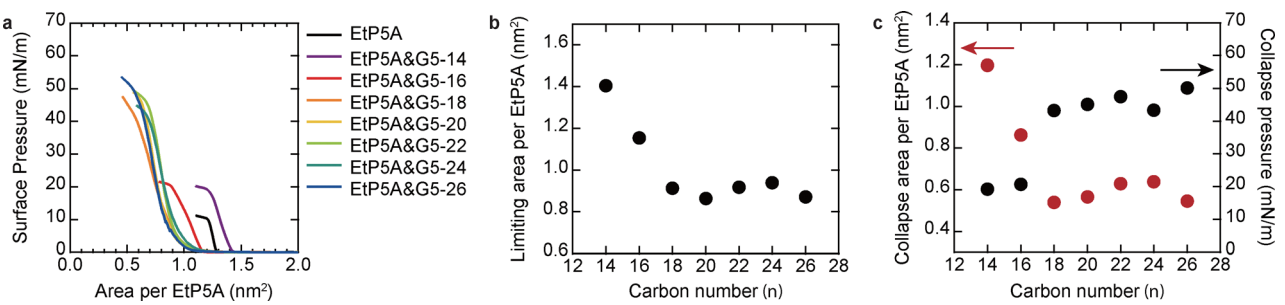

Fig. 2 Pseudorotaxane monolayers depending on the guest alkyl length. (a) π–A isotherms for mixtures of EtP5A and G5-*n*. (b) Correlation between extrapolated limiting area per EtP5A molecule and guest carbon number. (c) Characteristics of monolayer collapse for mixtures of EtP5A and G5-*n*.

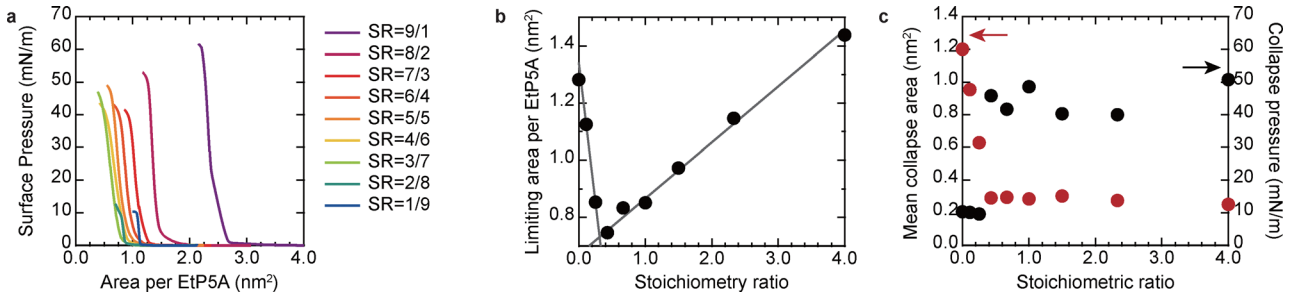

Fig. 3 Stoichiometric analysis of pseudorotaxane at the air–water interface. (a) π–A isotherms for mixtures of EtP5A and G5-20. (b) Correlation between extrapolated limiting area per EtP5A molecule and stoichiometric ratio. (c) Characteristics of monolayer collapse for mixtures of EtP5A and G5-20.

M. I. and Y. N. conducted comprehensive experiments and analyses, with the support of Y. Y. The synthesis of pillararenes was carried out by K. O. and T. S. under the supervision of T. O. The MAIRS measurements were overseen by T. H. and N. S. This study was conducted by K. A. and H. S., and T. M. M. I. was supported by JST, the establishment of university fellowships towards the creation of science technology innovation (Grant Number: JPMJFS2144). This work was also supported by KAKENHI (Grant Numbers: JP25H00898, JP23H05459 and JP23K04703). The calculations in this study were performed on the Numerical Materials Simulator at NIMS.

Data availability

The data supporting this article have been included as part of the ESI.†

Conflicts of interest

There are no conflicts to declare.

References

1 M. Xue, Y. Yang, X. Chi, X. Yan and F. Huang, *Chem. Rev.*, 2015, **115**, 7398–7501.
2 J. D. Badjic, V. Balzani, A. Credi, S. Silvi and J. F. Stoddart, *Science*, 2004, **303**, 1845–1849.
3 Y. Liu, A. H. Flood, P. A. Bonvallet, S. A. Vignon, B. H. Northrop, H.-R. Tseng, J. O. Jeppesen, T. J. Huang, B. Brough, M. Baller, S. Magonov, S. D. Solares, W. A. Goddard, C.-M. Ho and J. F. Stoddart, *J. Am. Chem. Soc.*, 2005, **127**, 9745–9759.
4 E. Katz, O. Lioubashevsky and I. Willner, *J. Am. Chem. Soc.*, 2004, **126**, 15520–15532.
5 M. J. Langton and P. D. Beer, *Acc. Chem. Res.*, 2014, **47**, 1935–1949.
6 S.-Y. Chou, H. Masai, M. Otani, H. V. Miyagishi, G. Sakamoto, Y. Yamada, Y. Kinoshita, H. Tamiaki, T. Katase and H. Ohta, *et al.*, *Appl. Catal., B*, 2023, **327**, 122373.
7 P. Wu, B. Dharmadhikari, P. Patra and X. Xiong, *Nanoscale Adv.*, 2022, **4**, 3418–3461.
8 O. N. OliveiraJr, L. Caseli and K. Ariga, *Chem. Rev.*, 2022, **122**, 6459–6513.
9 T. Ogoshi, S. Kanai, S. Fujinami, T.-A. Yamagishi and Y. Nakamoto, *J. Am. Chem. Soc.*, 2008, **130**, 5022–5023.
10 T. Ogoshi, T.-a Yamagishi and Y. Nakamoto, *Chem. Rev.*, 2016, **116**, 7937–8002.
11 M. Xue, Y. Yang, X. Chi, Z. Zhang and F. Huang, *Acc. Chem. Res.*, 2012, **45**, 1294–1308.
12 T. Ogoshi, R. Sueto, Y. Hamada, K. Doitomi, H. Hirao, Y. Sakata, S. Akine, T. Kakuta and T.-A. Yamagishi, *Chem. Commun.*, 2017, **53**, 8577–8580.
13 S. Dong, J. Yuan and F. Huang, *Chem. Sci.*, 2014, **5**, 247–252.
14 X.-Q. Wang, W. Wang, W.-J. Li, L.-J. Chen, R. Yao, G.-Q. Yin, Y.-X. Wang, Y. Zhang, J. Huang and H. Tan, *et al.*, *Nat. Commun.*, 2018, **9**, 3190.
15 A. N. Kursunlu, Y. Acikbas, M. Ozmen, M. Erdogan and R. Capan, *Analyst*, 2017, **142**, 3689–3698.
16 A. N. Kursunlu, Y. Acikbas, M. Ozmen, M. Erdogan and R. Capan, *Colloids Surf., A*, 2019, **565**, 108–117.
17 J. Umemura, T. Kamata, T. Kawai and T. Takenaka, *J. Phys. Chem.*, 1990, **94**, 62–67.
18 A. Modlinska and D. Bauman, *Int. J. Mol. Sci.*, 2011, **12**, 4923–4945.
19 N. Shioya, T. Mori, K. Ariga and T. Hasegawa, *Jpn. J. Appl. Phys.*, 2024, **63**, 060102.
20 N. Shioya, M. Yoshida, M. Fujii, T. Shimoaka, R. Miura, S. Maruyama and T. Hasegawa, *J. Phys. Chem. Lett.*, 2022, **13**, 11918–11924.
21 N. Shioya, M. Yoshida, M. Fujii, K. Eda and T. Hasegawa, *J. Am. Chem. Soc.*, 2024, **146**, 32032–32039.
22 M. Ishii, T. Mori, W. Nakanishi, J. P. Hill, H. Sakai and K. Ariga, *ACS Nano*, 2020, **14**, 13294–13303.
23 T. Ogoshi, S. Takashima and T.-A. Yamagishi, *J. Am. Chem. Soc.*, 2015, **137**, 10962–10964.
24 T. Ogoshi, K. Saito, R. Sueto, R. Kojima, Y. Hamada, S. Akine, A. M. P. Moeljadi, H. Hirao, T. Kakuta and T.-A. Yamagishi, *Angew. Chem., Int. Ed.*, 2018, **57**, 1592–1595.
25 S. Ohtani, K. Onishi, K. Wada, T. Hirohata, S. Inagi, J. Pirillo, Y. Hijikata, M. Mizuno, K. Kato and T. Ogoshi, *Adv. Funct. Mater.*, 2024, **34**, 2312304.